Open access • Journal Article • DOI:10.1038/NATURE11508

Long non-coding antisense RNA controls Uchl1 translation through an embedded SINEB2 repeat — Source link

Claudia Carrieri, Laura Cimatti, Marta Biagioli, Marta Biagioli ...+15 more authors

Institutions: International School for Advanced Studies, Harvard University, AREA Science Park, University of Trieste ...+2 more institutions

Published on: 15 Nov 2012 - Nature (Nature Publishing Group)

Topics: Sense strand, Antisense RNA, Sense (molecular biology), RNA and Transcription (biology)

LETTER

doi:10.1038/nature11508

Long non-coding antisense RNA controls *Uchl1* translation through an embedded SINEB2 repeat

Claudia Carrieri[1]*, Laura Cimatti[1]*, Marta Biagioli[1,2], Anne Beugnet[3], Silvia Zucchelli[1,2], Stefania Fedele[1], Elisa Pesce[3], Isidre Ferrer[4], Licio Collavin[5,6], Claudio Santoro[7], Alistair R. R. Forrest[8], Piero Carninci[8], Stefano Biffo[3,9], Elia Stupka[10] & Stefano Gustincich[1,2]

Most of the mammalian genome is transcribed[1–3]. This generates a vast repertoire of transcripts that includes protein-coding messenger RNAs, long non-coding RNAs (lncRNAs) and repetitive sequences, such as SINEs (short interspersed nuclear elements). A large percentage of ncRNAs are nuclear-enriched with unknown function[4]. Antisense lncRNAs may form sense–antisense pairs by pairing with a protein-coding gene on the opposite strand to regulate epigenetic silencing, transcription and mRNA stability[5–10]. Here we identify a nuclear-enriched lncRNA antisense to mouse ubiquitin carboxy-terminal hydrolase L1 (*Uchl1*), a gene involved in brain function and neurodegenerative diseases[11]. Antisense *Uchl1* increases UCHL1 protein synthesis at a post-transcriptional level, hereby identifying a new functional class of lncRNAs. Antisense *Uchl1* activity depends on the presence of a 5′ overlapping sequence and an embedded inverted SINEB2 element. These features are shared by other natural antisense transcripts and can confer regulatory activity to an artificial antisense to green fluorescent protein. Antisense *Uchl1* function is under the control of stress signalling pathways, as mTORC1 inhibition by rapamycin causes an increase in UCHL1 protein that is associated to the shuttling of antisense *Uchl1* RNA from the nucleus to the cytoplasm. Antisense *Uchl1* RNA is then required for the association of the overlapping sense protein-coding mRNA to active polysomes for translation. These data reveal another layer of gene expression control at the post-transcriptional level.

To discover non-coding antisense transcripts of sense–antisense (S–AS) pairs expressed in the brain, the mouse syntenic loci of genes involved in neurodegenerative diseases were identified computationally and examined in the Ensembl browser (http://www.ensembl.org). The FANTOM2 clone 6430596G22 was classified as a spliced antisense lncRNA of the *Uchl1* gene[11]; we refer to this as antisense *Uchl1*. UCHL1 is a neuron-restricted protein that acts as a deubiquitinating enzyme, ubiquitin ligase or monoubiquitin stabilizer[12]. An in-frame deletion in the *Uchl1* gene, as in gracile axonal dystrophy mice, leads to ataxia and axonal degeneration. Although an association of *UCHL1* gene mutations to familial Parkinson's disease has not been confirmed in independent families, oxidative inactivation of UCHL1 protein has been reported in Parkinson's disease and Alzheimer's disease brains[13–15].

Antisense *Uchl1* is a 5′ head-to-head transcript that initiates within the second intron of *Uchl1* and overlaps the first 73 nucleotides of the sense mRNA including the AUG codon. By 5′ rapid amplification of cDNA ends (RACE), the transcriptional start site (TSS) of antisense *Uchl1* was mapped to the second intron of *Uchl1* (Fig. 1a). The non-overlapping part of the transcript contains two embedded repetitive sequences, SINEB1 of the F1 subclass (Alu) and SINEB2 of the B3 subclass, identified by Repeatmasker[16–18]. The FANTOM2 clone spans a genomic region of 70 kilobases (kb) (Fig. 1a) and its genomic organization is conserved in mammals (Supplementary Fig. 1a).

Sense and antisense *Uchl1* expression in mouse and human tissues was similar (Fig. 1b and Supplementary Fig. 1b). In the mouse, antisense *Uchl1* RNA was highly expressed in the ventral midbrain (Fig. 1b) and in the MN9D dopaminergic cell line (data not shown). Mature *Uchl1* mRNA was observed mainly in the cytoplasm of dopaminergic neurons, whereas antisense *Uchl1* was enriched in the nucleus (Fig. 1c and Supplementary Fig. 2). Antisense *Uchl1* expression was confirmed by qRT–PCR from dopaminergic neurons purified with laser capture microdissection (LCM, Supplementary Fig. 3).

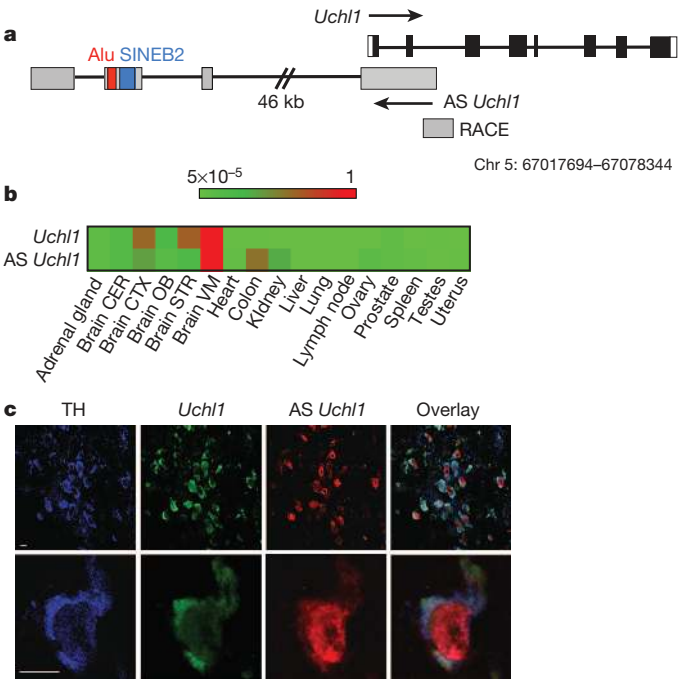

Figure 1 | Expression of antisense *Uchl1* in dopaminergic neurons. a, *Uchl1*/antisense (AS) *Uchl1* genomic organization. *Uchl1* exons are in black; 3′ and 5′ UTRs are in white; antisense *Uchl1* exons are grey; repetitive elements are in red (Alu) and blue (SINEB2). Introns are indicated as lines. **b**, Quantitative expression of *Uchl1* and antisense *Uchl1* in mouse tissues ($\Delta\Delta Ct/\Delta\Delta Ct_{max}$). CER, cerebellum; CTX, cortex; OB, olfactory bulb; STR, striatum; VM, ventral midbrain. **c**, Antisense *Uchl1* (red) and *Uchl1* (green) transcripts are expressed in the nucleus and cytoplasm of TH-positive dopaminergic neurons of the substantia nigra (blue).

[1]Area of Neuroscience, International School for Advanced Studies (SISSA), via Bonomea 265, 34136 Trieste, Italy. [2]The Giovanni Armenise-Harvard Foundation Laboratory, via Bonomea 265, 34136 Trieste, Italy. [3]Laboratory of Molecular Histology and Cell Growth, DIBIT, San Raffaele Scientific Institute, Via Olgettina 58, 20132 Milan, Italy. [4]Institute of Neuropathology, IDIBELL-University Hospital of Bellvitge, Carrer Feixa Llarga sn, 08907 Hospitalet de Llobregat, Spain. [5]Laboratorio Nazionale Consorzio Interuniversitario Biotecnologie (LNCIB), Area Science Park, Padriciano 99, 34149 Trieste, Italy. [6]Department of Life Sciences (DSV), University of Trieste, via Giorgeri 1, 34129 Trieste, Italy. [7]Department of Health Sciences, University of Eastern Piedmont, Viale Solaroli 17, 28100 Novara, Italy. [8]Omics Science Center, RIKEN Yokohama Institute, 1-7-22 Suehiro-chô, Tsurumi-ku, Yokohama, Kanagawa 230-0045, Japan. [9]Department of Environmental and Life Sciences, University of Eastern Piedmont, Viale T. Michel 11, 15121 Alessandria, Italy. [10]Center for Translational Genomics and Bioinformatics, San Raffaele Scientific Institute, Via Olgettina 58, 20132 Milan, Italy.
*These authors contributed equally to this work.

Transient expression of antisense *Uchl1* in MN9D cells caused no significant change in endogenous *Uchl1* mRNA expression. Notably, a strong and reproducible upregulation of UCHL1 protein was detected within 24 h (Fig. 2a). When increasing amounts of antisense *Uchl1* were co-transfected with murine *Uchl1* into HEK cells, which do not express either transcript, dose-dependent UCHL1 protein upregulation was recorded in the absence of any significant change in the quantity of exogenous *Uchl1* mRNA (Fig. 2b). These data indicate that antisense *Uchl1* regulates UCHL1 expression at a post-transcriptional level.

Antisense *Uchl1* deletion constructs lacking the 5′ first exon (antisense *Uchl1*(Δ5′)) or the last three exons (antisense *Uchl1*(Δ3′)) failed to induce UCHL1 protein in MN9D and HEK cells, suggesting that both 5′ and 3′ components are important to antisense *Uchl1* function (Fig. 2c and Supplementary Fig. 4a). Targeted deletion of the region containing the embedded SINEB2 and Alu repetitive sequences (ΔAS) was also able to prevent UCHL1 protein induction. Deletion of each repetitive element separately revealed that SINEB2 is the functional unit required by antisense *Uchl1* for increasing UCHL1 protein synthesis (Fig. 2d). In all cases no change in *Uchl1* mRNA level was detected (Supplementary Fig. 4b). A mutant with a flipped SINEB2 sequence was unable to increase UCHL1 protein levels, thus proving the orientation-dependent activity of the SINEB2 domain embedded within antisense *Uchl1* (Fig. 2d). Importantly, an artificial construct containing the 73-nucleotide overlapping sequence immediately close to the repetitive elements in antisense *Uchl1*(Δ5′) increased UCHL1 levels as much as the full-length clone (Fig. 2e and Supplementary Fig. 4c).

We then considered whether other SINEB2-containing lncRNAs may post-transcriptionally regulate the expression of their protein-coding partner, on the basis of similar structural elements. The FANTOM3 collection of non-coding cDNAs was bioinformatically screened for natural antisense transcripts that contain SINEB2 elements of the B3 subclass in the correct orientation and 5′ head-to-head overlapping to a protein-coding gene. This identified 31 S–AS pairs similar to the *Uchl1*/antisense *Uchl1* structure (Supplementary Fig. 5). By sequence alignment, we chose antisense *Uxt* (4833404H03), antisense of ubiquitously expressed transcript (*Uxt*), as the one with the most similar SINEB2 elements (Fig. 3a). Transfection of antisense *Uxt* in MN9D cells elicited an increase of UXT protein level with no change in *Uxt* mRNA (Fig. 3b), indicating that antisense *Uxt* was similarly able to increase protein levels post-transcriptionally.

These data indicate a model whereby lncRNAs regulate protein synthesis through the combined activities of two domains. The 5′ antisense

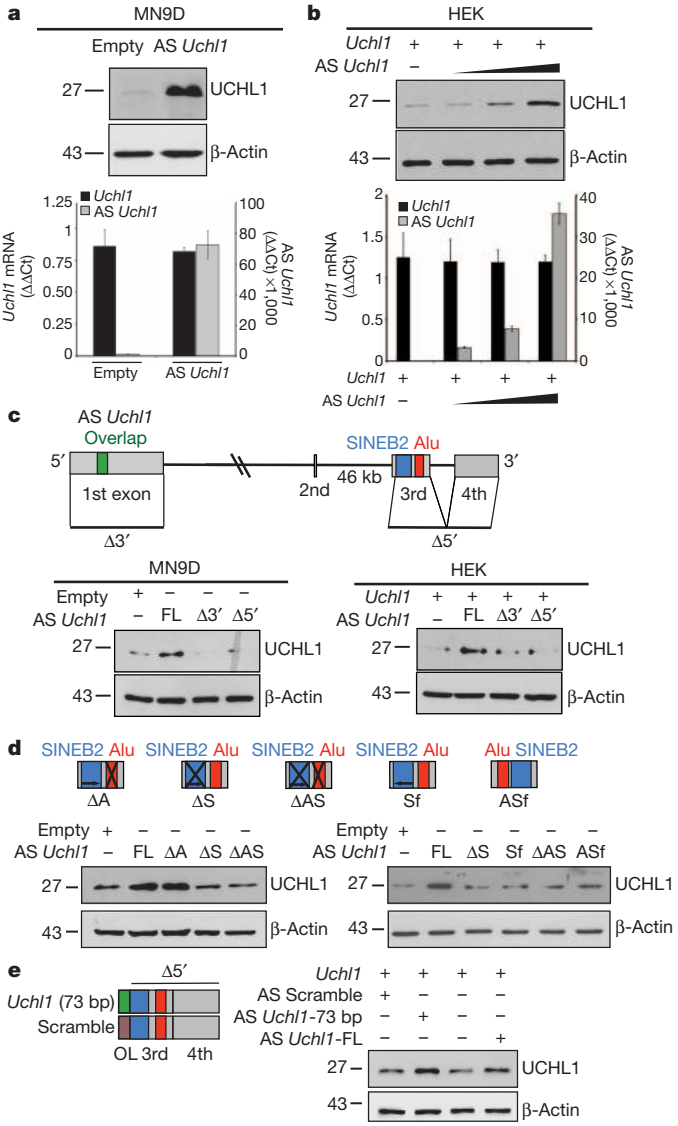

Figure 2 | Antisense *Uchl1* regulates UCHL1 protein levels via an embedded inverted SINEB2 element. **a**, Antisense *Uchl1*-transfected dopaminergic MN9D cells show increased levels of endogenous UCHL1 protein, with unchanged mRNA quantity. **b**, Increasing doses of transfected antisense *Uchl1* titrate UCHL1 protein but not mRNA levels in HEK cells. Data in **a** and **b** indicate mean ± s.d., $n \geq 3$. **c**, Full-length (FL) antisense *Uchl1* is required for regulating endogenous (MN9D cells, left panel) and overexpressed (HEK cells, right panel) UCHL1 protein levels. Scheme of Δ5′ or Δ3′ deletion mutants is shown. **d**, Inverted SINEB2 is sufficient to control endogenous UCHL1 protein levels in MN9D cells. Scheme of mutants is shown in 5′ to 3′ orientation. ΔA, ΔAlu; ΔS, ΔSINEB2; ΔAS, ΔAlu+SINEB2; Sf, SINEB2 flipped; ASf, Alu+SINEB2 flipped. **e**, A 73-bp overlap (OL) of antisense *Uchl1* is sufficient to increase UCHL1 in transfected HEK cells. Scheme of mutant and scramble control in 5′ to 3′ orientation. Units for numbers along the left of gels in **a**–**e** indicate kDa.

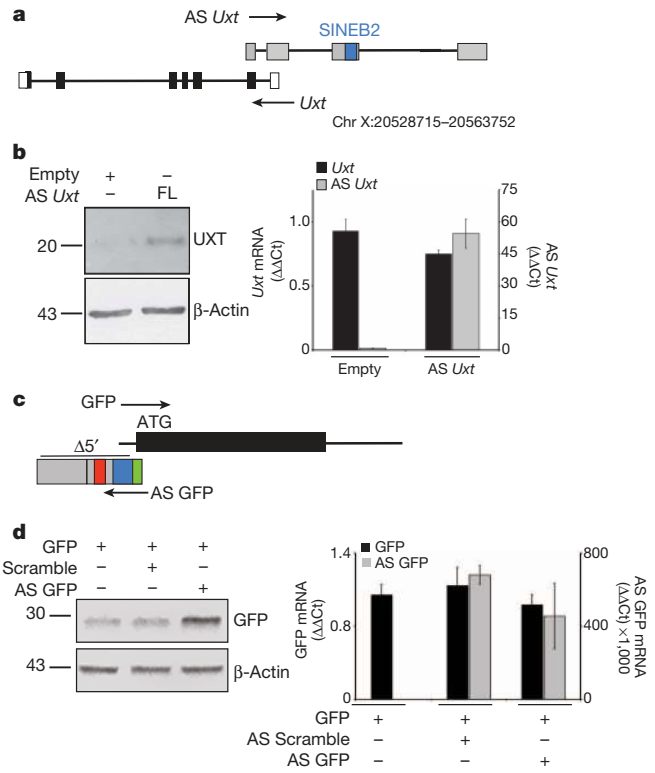

Figure 3 | Natural and synthetic antisense lncRNAs increase target protein levels. **a**, Scheme of *Uxt*/antisense *Uxt* genomic organization. **b**, Antisense *Uxt* increases endogenous UXT protein levels (left) without affecting RNA levels (right) in transfected MN9D cells. **c**, Scheme of antisense GFP construct. Δ5′ with repetitive elements (SINEB2, blue; Alu, red) and overlap (green) regions is indicated. **d**, Inverted SINEB2 plus the overlap sequence increase GFP levels in transfected cells. Data in **b** and **d** indicate mean ± s.d., $n \geq 3$.

region provides specificity for the sense target gene whereas the repetitive element confers the protein synthesis activation domain. The model predicts that by swapping the overlapping sequence one may increase the amount of proteins encoded by the mRNAs of choice acting at the post-transcriptional level. We thus synthesized a 72-nucleotide-long artificial sequence antisense to the AUG-containing region as transcribed from pEGFP, and inserted it into antisense *Uchl1*(Δ5′) to generate antisense GFP (Fig. 3c). Co-transfection of antisense GFP with pEGFP strongly increased GFP protein but not mRNA levels in HEK cells (Fig. 3d). When we pulsed cells with methionine for an hour and immunoprecipitated GFP, antisense GFP induced an increase in radioactively labelled, neo-synthesized GFP, without affecting mRNA levels (Supplementary Fig. 6).

To understand how the antisense *Uchl1* transcript operates and the physiological conditions in which it might act, we assayed several stimuli and/or drugs for their ability to modulate UCHL1 protein expression. Inhibition of mTORC1 signalling favoured an increase in UCHL1 levels in a range from 1.5- to 2.5-fold (Fig. 4a). This effect was evident with as low as 20 nM rapamycin (Supplementary Fig. 7) and was concomitant with dephosphorylation of mTOR targets p70S6K and 4E-BP1. Furthermore, the effect was not due to a stabilization of the protein, as co-application of cycloheximide decreased UCHL1 protein levels (Supplementary Fig. 8a). These data are surprising because rapamycin impairs formation of the CAP-dependent complex and hence translation of highly structured mRNAs[19]. However, in agreement with previous reports, in our experimental settings mTORC1 inhibition only slightly impairs the global rate of translation (Supplementary Fig. 8b). Under these conditions, it has been proposed that rapamycin may affect competition among different mRNAs[20]. If so, we proposed that inhibition of the CAP complex formation favours the translation of *Uchl1* mRNA with a mechanism that requires antisense *Uchl1*.

To test this model, we used two complementary approaches to establish a loss-of-function phenotype. First, we downregulated antisense *Uchl1* levels with short hairpin RNA (shRNA) targeting its promoter region. MN9D cells constitutively expressing shRNA for antisense *Uchl1* did not show any changes in UCHL1 protein levels upon rapamycin treatment, whereas scramble control cells showed UCHL1 upregulation as in the parental line (Fig. 4b). Dephosphorylation of p70S6K and 4E-BP1 proved that rapamycin inhibited mTOR activity as expected. We then exploited the dominant-negative property of an antisense *Uchl1* mutant lacking the SINEB2 repeat element. Overexpression of antisense *Uchl1*(ΔSINEB2) inhibited the ability of full-length antisense *Uchl1* to increase protein levels (Supplementary Fig. 9). Upon rapamycin treatment, cells stably expressing antisense *Uchl1*(ΔSINEB2) did not show any UCHL1 protein induction despite dephosphorylation of mTOR targets (Fig. 4c). These complementary experiments prove that functional antisense expression is required for UCHL1 protein increase elicited by rapamycin.

Because antisense *Uchl1* transcript is enriched in the nucleus of dopaminergic neurons, we measured antisense *Uchl1* and *Uchl1* RNA content in the nucleus and cytoplasm of MN9D cells upon rapamycin treatment. As shown in Fig. 4d, rapamycin substantially increased antisense *Uchl1* concentration in the cytoplasmic fraction. This effect was confirmed by a concomitant decrease in its nuclear steady-state levels, and by the absence of any *de novo* transcription. The total content of primary and spliced transcripts remained constant (data not shown). *Uchl1* mRNA showed no change in subcellular distribution, *de novo* transcription or total cellular content. These data demonstrate that antisense *Uchl1* localization can be regulated by the mTOR pathway, and its cytoplasmic level correlates with the expression of UCHL1 protein.

We therefore monitored the association of *Uchl1* mRNA with polysomes to assess the role of translation in antisense *Uchl1*-mediated UCHL1 protein induction. Fractionated MN9D cell extracts were used to measure the recruitment of *Uchl1* mRNA on polysomes by

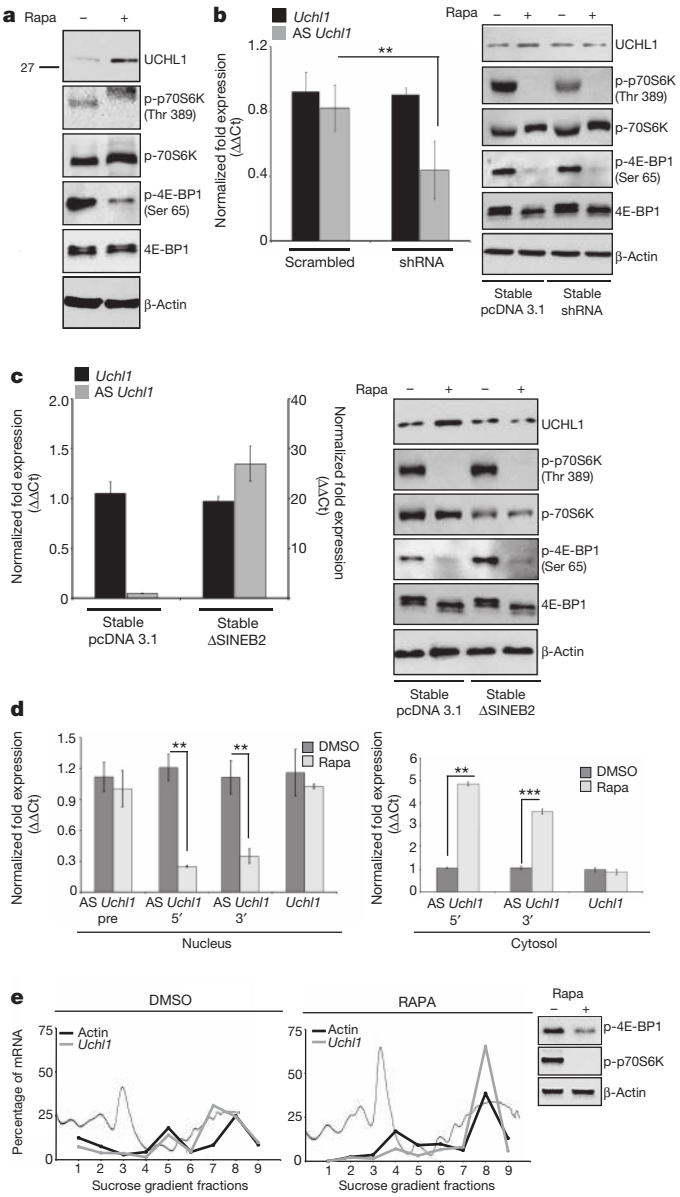

Figure 4 | Antisense *Uchl1* mediates UCHL1 protein induction by rapamycin. **a**, UCHL1 protein level is increased in rapamycin-treated MN9D cells. Rapamycin inhibition of mTOR pathway is verified with anti-p-p70S6K and anti-p-4E-BP1 antibodies. **b**, Silencing antisense *Uchl1* transcription (shRNA) in MN9D cells inhibits rapamycin-induced UCHL1 protein level. Left, mRNA levels; right, protein levels. **c**, Deletion of embedded SINEB2 (ΔSINEB2) is sufficient to inhibit rapamycin-induced UCHL1 protein upregulation. **d**, Antisense *Uchl1* translocates to the cytoplasm upon rapamycin treatment in MN9D cells. mRNA levels were measured with 5′ or 3′ primers. Data in **b**–**d** indicate mean ± s.d., $n \geq 3$. $^{**}P < 0.01$; $^{***}P < 0.005$. **e**, Rapamycin increases *Uchl1* mRNA in heavy polysomes; the absorbance profile is outlined in the background of each plot.

qRT–PCR and northern blotting (Fig. 4e and Supplementary Fig. 10). In basal conditions, *Uchl1* mRNA was associated with translating ribosomes. Rapamycin treatment induced a shift of *Uchl1* mRNA to heavier polysomes, consistent with an enhanced rate of translation initiation; this increase of *Uchl1* mRNA association to heavier polysomes did not occur in cells overexpressing the dominant-negative form of antisense *Uchl1* (Supplementary Fig. 11).

Antisense *Uchl1* is the representative member of a new functional class of lncRNAs that are part of S–AS pairs in the mammalian genome that require overlap at the 5′ end and the action of a SINEB2 repeat. This new function for SINEB2 sequences in the cytoplasm adds to their

well-established role in the nucleus as inhibitors of RNA polymerase II[16]. Stress-dependent nucleocytoplasmic shuttling of lncRNAs may be a common strategy to regulate translation, as CTN-RNA, another nuclear-retained lncRNA, was found to have a cryptic protein-coding sequence at its 3′ end when in the cytoplasm[21].

It is intriguing that this nuclear lncRNA-mediated mechanism for post-transcriptional control of gene expression is active when CAP-dependent translation is inhibited by rapamycin. This drug blocks mTORC1 kinase, which activates the eIF4F complex[19,22]. However, some mRNAs escape mTORC1 inhibition by being able to be recruited to ribosomes in an eIF4F-independent manner for presenting complex mRNA loops that function as internal ribosomal entry sites (IRES)[23]. Indeed, IRES-mediated translation is prominent in conditions of stress or growth factor inhibition and its alteration affects processes such as tumorigenesis[22,24]. In genetic and neurochemical models of Parkinson's disease, mTORC1 inhibition protects dopaminergic neurons from apoptosis[25,26].

Antisense lncRNA-mediated translation may be another mechanism to maintain synthesis of pro-survival proteins, such as UCHL1, that are involved in rapamycin neuroprotective function and more generally in cellular response to stress. This mechanism may represent the outcome of an evolutionary pressure on the genomic organization of anti-stress elements to favour gene-specific regulation of translation when CAP-dependent initiation is reduced. Finally, natural and synthetic antisense transcripts with embedded repetitive elements may represent molecular tools to increase translation of selected mRNAs, defining a potential new class of RNA therapeutics.

METHODS SUMMARY

5′ RACE for antisense *Uchl1* was performed with Gene Racer (Invitrogen). Double-fluorescence *in situ* hybridization of biotin- and digoxigenin-labelled probes was detected using fluorochrome-conjugated reagents. Images were captured with Confocal Laser Microscopy (LEICA). Expression of antisense *Uchl1* was performed on neuronal cells lines and dopaminergic neurons purified with LCM from TH-GFP mice. Cell lines were cultured under standard conditions. shRNA targeting the promoter of antisense *Uchl1* was cloned in pSUPERIOR.Neo.GFP vector (Oligo Engine). Polysomes were prepared by sucrose gradient and associated *Uchl1* mRNA was measured by qRT–PCR and northern blotting.

Full Methods and any associated references are available in the online version of the paper.

Received 3 December 2010; accepted 14 August 2012.
Published online 14 October 2012.

1. Birney, E. *et al.* Identification and analysis of functional elements in 1% of the human genome by the ENCODE pilot project. *Nature* **447,** 799–816 (2007).
2. The FANTOM Consortium. The transcriptional landscape of the mammalian genome. *Science* **309,** 1559–1563 (2005).
3. Kapranov, P., Willingham, A. T. & Gingeras, T. R. Genome-wide transcription and the implications for genomic organization. *Nature Rev. Genet.* **8,** 413–423 (2007).
4. Kapranov, P. *et al.* RNA maps reveal new RNA classes and a possible function for pervasive transcription. *Science* **316,** 1484–1488 (2007).
5. Beltran, M. *et al.* A natural antisense transcript regulates Zeb2/Sip1 gene expression during Snail1-induced epithelial-mesenchymal transition. *Genes Dev.* **22,** 756–769 (2008).
6. Ebralidze, A. K. *et al.* PU.1 expression is modulated by the balance of functional sense and antisense RNAs regulated by a shared cis-regulatory element. *Genes Dev.* **22,** 2085–2092 (2008).
7. Hastings, M. L., Ingle, H. A., Lazar, M. A. & Munroe, S. H. Post-transcriptional regulation of thyroid hormone receptor expression by cis-acting sequences and a naturally occurring antisense RNA. *J. Biol. Chem.* **275,** 11507–11513 (2000).
8. Huarte, M. *et al.* A large intergenic noncoding RNA induced by p53 mediates global gene repression in the p53 response. *Cell* **142,** 409–419 (2010).
9. Katayama, S. *et al.* Antisense transcription in the mammalian transcriptome. *Science* **309,** 1564–1566 (2005).
10. Spigoni, G., Gedressi, C. & Mallamaci, A. Regulation of Emx2 expression by antisense transcripts in murine cortico-cerebral precursors. *PLoS ONE* **5,** e8658 (2010).
11. Setsuie, R. & Wada, K. The functions of UCH-L1 and its relation to neurodegenerative diseases. *Neurochem. Int.* **51,** 105–111 (2007).
12. Liu, Y., Fallon, L., Lashuel, H. A., Liu, Z. & Lansbury, P. T. Jr. The UCH-L1 gene encodes two opposing enzymatic activities that affect α-synuclein degradation and Parkinson's disease susceptibility. *Cell* **111,** 209–218 (2002).
13. Barrachina, M. *et al.* Reduced ubiquitin C-terminal hydrolase-1 expression levels in dementia with Lewy bodies. *Neurobiol. Dis.* **22,** 265–273 (2006).
14. Barrachina, M. *et al.* Amyloid-β deposition in the cerebral cortex in dementia with Lewy bodies is accompanied by a relative increase in AβPP mRNA isoforms containing the Kunitz protease inhibitor. *Neurochem. Int.* **46,** 253–260 (2005).
15. Choi, J. *et al.* Oxidative modifications and down-regulation of ubiquitin carboxyl-terminal hydrolase L1 associated with idiopathic Parkinson's and Alzheimer's diseases. *J. Biol. Chem.* **279,** 13256–13264 (2004).
16. Nishihara, H., Smit, A. F. & Okada, N. Functional noncoding sequences derived from SINEs in the mammalian genome. *Genome Res.* **16,** 864–874 (2006).
17. Ponicsan, S. L., Kugel, J. F. & Goodrich, J. A. Genomic gems: SINE RNAs regulate mRNA production. *Curr. Opin. Genet. Dev.* **20,** 149–155 (2010).
18. Quentin, Y. Fusion of a free left Alu monomer and a free right Alu monomer at the origin of the Alu family in the primate genomes. *Nucleic Acids Res.* **20,** 487–493 (1992).
19. Andrei, M. A. *et al.* A role for eIF4E and eIF4E-transporter in targeting mRNPs to mammalian processing bodies. *RNA* **11,** 717–727 (2005).
20. Merrick, W. C. Eukaryotic protein synthesis: still a mystery. *J. Biol. Chem.* **285,** 21197–21201 (2010).
21. Prasanth, K. V. *et al.* Regulating gene expression through RNA nuclear retention. *Cell* **123,** 249–263 (2005).
22. Holcik, M. & Sonenberg, N. Translational control in stress and apoptosis. *Nature Rev. Mol. Cell Biol.* **6,** 318–327 (2005).
23. Gilbert, W. V. Alternative ways to think about cellular internal ribosome entry. *J. Biol. Chem.* **285,** 29033–29038 (2010).
24. Yoon, A. *et al.* Impaired control of IRES-mediated translation in X-linked dyskeratosis congenita. *Science* **312,** 902–906 (2006).
25. Malagelada, C., Jin, Z. H., Jackson-Lewis, V., Przedborski, S. & Greene, L. A. Rapamycin protects against neuron death in *in vitro* and *in vivo* models of Parkinson's disease. *J. Neurosci.* **30,** 1166–1175 (2010).
26. Santini, E., Heiman, M., Greengard, P., Valjent, E. & Fisone, G. Inhibition of mTOR signaling in Parkinson's disease prevents L-DOPA-induced dyskinesia. *Sci. Signal.* **2,** ra36 (2009).

Supplementary Information is available in the online version of the paper.

Acknowledgements We thank S.G. laboratory members for thought-provoking discussions and C. Leonesi for technical help. We thank F. Persichetti, A. Mallamaci, E. Calautti, S. Saoncella, A. Lunardi, D. De Pietri Tonelli, R. Sanges, M. E. MacDonald and T. Perlmann for support and discussions; and M. J. Zigmond and B. Joseph for sharing the MN9D cell line. This work was supported by the FP7 Dopaminet to S.G., E.S. and P.C., by The Giovanni Armenise-Harvard Foundation to S.G. and by the Compagnia di San Paolo to S.B.

Author Contributions C.C. designed and performed the experiments, and analysed the results; L.Ci. designed and performed the experiments, and analysed the results; M.B. designed and performed the experiments, and analysed the results; A.B. prepared polysomes; S.Z. designed the experiments, analysed the results and wrote the manuscript; S.F. carried out qRT–PCR on polysome fractions and the pulse labelling experiment; E.P. prepared polysomes and carried out northern blotting; I.F. analysed the results; L.Co. designed the experiments and analysed the results; C.S. analysed the data and discussed the results; A.R.R.F. performed bioinformatic analysis for the identification of SINEB2 and family members and designed ΔAlu and ΔSINEB2 mutants; P.C. provided reagents, experimental design and managing; S.B. designed polysome experiments, analysed the data and wrote the manuscript; E.S. performed bioinformatic analysis for the identification of S–AS pairs, designed experiments for the analysis of antisense *Uchl1* expression and analysed the results; S.G. designed the experiments, analysed the results and wrote the paper.

Author Information Reprints and permissions information is available at www.nature.com/reprints. The authors declare competing financial interests: details are available in the online version of the paper. Readers are welcome to comment on the online version of the paper. Correspondence and requests for materials should be addressed to S.G. (gustinci@sissa.it).

METHODS

Oligonucleotides. The complete list of oligonucleotides used for cloning and for quantitative real-time PCR experiments is included in Supplementary Information (Supplementary Fig. 12).

Plasmids. Full-length DNA sequence of antisense *Uchl1* was amplified via fusion PCR starting from RACE fragment and FANTOM clone 6430596G22 (GenBank AK078321.1) with forward mouse antisense *Uchl1* FL and reverse mouse antisense *Uchl1* FL primers.

Mouse *Uchl1* mRNA was subcloned from FANTOM clone 2900059O22 (GenBank AK013729.1) in the unique PmeI site of pcDNA3.1.

cDNA sequence of human antisense *UCHL1* was amplified from a sample of human brain total RNA (Clontech, 636530) with the primers human 5′F and human 3′R.

Oligonucleotides that target the sequence −14/+3 around the TSS of antisense *Uchl1* were annealed and cloned into pSUPERIOR.Neo.GFP vector (OligoEngine) in the BglII/XhoI site. Scrambled sequence was also cloned and used as control.

The antisense *Uchl1* 5′ deletion mutant (Δ5′) was generated by PCR using the oligonucleotides forward mouse antisense *Uchl1*(Δ5′) and reverse mouse antisense *Uchl1* FL. PCR fragment was cloned in the unique EcoRI site in pcDNA3.1.

The antisense *Uchl1* 3′ deletion mutant (Δ3′) was generated by PCR using the forward mouse antisense *Uchl1* FL and reverse mouse antisense *Uchl1*(Δ3′) primers and cloned in the unique EcoRI site in pcDNA3.1.

The antisense *Uchl1*(ΔAS) (ΔAlu + SINEB2) mutant was obtained by subsequent cloning of PCR fragment I (NheI–EcoRI site) and PCR fragment II (EcoRI–HindIII site) into pcDNA3.1. Primers forward mouse antisense *Uchl1* FL Nhe and reverse pre-SINE B2 EcoRI were used to generate fragment I; primers forward post-ALU EcoRI and reverse mouse antisense FL HindIII were used for PCR fragment II.

The antisense *Uchl1*(ΔA) (ΔAlu, 1000–1045) mutant was generated with a similar strategy to antisense *Uchl1*(ΔAS). Forward mouse antisense *Uchl1* FL NheI and reverse pre-ALU EcoRI were used for PCR fragment I; forward post-ALU and reverse mouse antisense FL HindIII for PCR fragment II.

The antisense *Uchl1*(ΔS) (ΔSINEB2, 764–934) mutant was obtained with a similar strategy to antisense *Uchl1*(ΔAS). Oligonucleotides forward mouse AS *Uchl1* FL NheI and reverse pre-SINE B2 EcoRI for fragment I; forward post-SINE B2 EcoRI and reverse mouse AS FL HindIII for fragment II.

For antisense *Uchl1*(ASf) (Alu + SINEB2 flipped), PCR fragment obtained with the primers forward SINEB2 inside and reverse Alu flip was cloned in the unique EcoRI site of antisense *Uchl1*(ΔAS).

For antisense *Uchl1*(Sf) (SINEB2 flipped), PCR fragment obtained with forward SINE B2 inside and reverse SINE flip oligonucleotides was cloned in the unique EcoRI site of antisense *Uchl1* ΔSINEB2.

For antisense *Uchl1*(73 bp), the method of 'annealing and primer extension' of two 3′-end overlapping oligonucleotides was used to generate the 73-bp antisense *Uchl1* overlap region. Annealed fragment was obtained with antisense *Uchl1* 73 bp forward and antisense *Uchl1* 73 bp reverse. Fragment was digested with XhoI and EcoRV and ligated into antisense *Uchl1* Δ5′ plasmid.

The antisense SCR 73-bp mutant was obtained with a similar strategy as antisense *Uchl1*(73 bp). The annealing extension was performed with oligonucleotides with scramble (SCR) sequence (antisense SCR forward and antisense SCR reverse).

Full-length mouse antisense *Uxt* was amplified by PCR starting from FANTOM clone 4833404H03 (GenBank AK029359.1) with specific primers (forward mouse antisense *Uxt* and reverse mouse antisense *Uxt*). PCR fragment was subcloned into pcDNA3.1 using XbaI and HindIII restriction enzymes.

The antisense GFP plasmid was generated with a similar strategy as antisense *Uchl1*(73 bp). Seventy-two base pairs corresponding to nucleotide −40/+32 with respect to the ATG of GFP sequence in pEGFP-C2 vector (Clontech) were chosen as target sequence for artificial antisense DNA generation. For annealing, the GFP antisense forward and GFP antisense reverse primers were used.

Cells. MN9D cells were obtained from M. J. Zigmond. Cells were seeded in 100-mm dishes in Dulbecco's modified Eagle's (DMEM) medium containing 10% fetal bovine serum (Invitrogen) supplemented with penicillin (50 units ml^{-1}) and streptomycin (50 units ml^{-1}). For experiments, cells were plated in poly-L-lysine (P2636, Sigma) coated dishes and grown overnight. Approximately 50% confluent cells were treated with 1 μM rapamycin (R0395, Sigma) or DMSO vehicle for 45 min.

For the establishment of stable cell lines (shRNA -15/+4, shRNA scrambled, pcDNA 3.1- and AS Uchl1ΔSINEB2), MN9D cells were seeded in 100-mm Petri dishes and transfected with Lipofectamine 2000 (Invitrogen) according to the manufacturer's instruction. Stable clones were selected by 500 μM neomycin (N1142, Sigma). HEK cells (Sigma) were cultured under standard condition in DMEM containing 10% fetal bovine serum supplemented with antibiotics. Transient transfections were done with Lipofectamine 2000 (Invitrogen). For all experiments, S and AS plasmids were transfected at 1:6 ratio.

Animal handling. All animal experiments were performed in accordance with European guidelines for animal care and following SISSA Ethical Committee permissions. Mice were housed and bred in SISSA/CBM non-SPF animal facility, with 12 h dark/light cycles and controlled temperature and humidity. Mice had *ad libitum* access to food and water. C57BL/6 male mice ($n = 5$), 8–10 weeks old, were used for *in situ* hybridization experiments. Laser capture microdissection (LCM) of dopaminergic neurons was performed on 8–10-week-old male TH-GFP/21-31 mice ($n = 3$). Intra-cardiac perfusions were done under total anaesthesia.

RACE and multiplex RT–PCR. The 5′ UTR of antisense *Uchl1* was amplified by RACE PCR (GeneRacer, Invitrogen) by MN9D total RNA and cloned into pGEM-T Easy vector (Promega).

qRT–PCR. Total RNA was extracted from cells and mouse tissue samples (adrenal gland, cerebellum, cortex, olfactory bulb, striatum, ventral midbrain, heart, colon, kidney, lung, lymph node, ovary, prostate, spleen, testis, uterus) using Trizol reagent (Invitrogen) according to the manufacturer's instruction. An RNA panel of 20 different normal human tissues (pools consist of at least three tissue donors with full documentation on age, sex, race, cause of death) was obtained from Ambion (AM6000). All RNA samples were subjected to DNase I treatment (Ambion). A total of 1 μg of RNA was subjected to retrotranscription using iScript cDNA synthesis kit (BioRad) and Real Time qRT–PCR was carried out using SYBR green fluorescence dye (2× iQ5 SYBR Green supermix, BioRad). TATA-binding protein (TBP) and RNA polymerase II (RPII) were used as housekeeping genes to normalize different mouse and human tissues as tested by the GeNorm program, version 3.5 (http://medgen.ugent.be/genorm/)[27]. GAPDH and β-actin were used as normalizing controls in all the other qRT–PCR experiments. The amplified transcripts were quantified using the comparative Ct method and the differences in gene expression were presented as normalized fold expression (ΔΔCt). All of the experiments were performed in duplicate. A heat map graphical representation of rescaled normalized fold expression ($\Delta\Delta Ct/\Delta\Delta Ct_{max}$) was obtained by using Matrix2png (http://www.bioinformatics.ubc.ca/matrix2png/). A list of oligonucleotides used for qRT–PCR experiments is in Supplementary Fig. 12.

LCM technology. For LCM, regions of midbrain from TH-GFP/21-31 mice were dissected and incubated in 1× Zincfix solution for 6 h. They were then cryoprotected in 30% sucrose solution at 4 °C overnight, embedded in Neg-50 section medium, snap-frozen and left to equilibrate in a cryostat chamber at −21 °C for 1 h before sectioning, as described earlier[28]. Cryostat 14 μm midbrain coronal sections were thaw-mounted on Superfrost plus glass slides (Mezzle-Glasser) and dopaminergic GFP^+ cells were gathered via LCM and collected in microfuge (PALM adhesive caps). RNA was immediately extracted using the Absolutely RNA Nanoprep kit (Stratagene), eluted in RNase/DNase free water (Ambion) and retro-transcribed.

Two-colour *in situ* hybridization. After perfusion with 4% formaldehyde, mouse brain was cryoprotected overnight in 30% sucrose. *In situ* hybridization was performed on cryostat slices (16 μm). Sense and antisense probes were generated by *in vitro* transcription from the cDNA encoding the distal 600 bp of mouse *Uchl1* cDNA and the last 1,000 bp of mouse antisense *Uchl1*. The probes for *Uchl1* and antisense *Uchl1* were labelled with digoxigenin (DIG labelling, Roche) and biotin (BIO-labelling mix, Roche), respectively. Incorporation of biotin and digoxigenin was checked via a northern blot assay. *In situ* hybridization was performed as described previously[29]. Slices were pre-treated with 3% hydrogen peroxide for 30 min. Hybridization was performed with probes at a concentration of 1 μg ml^{-1} (*Uchl1*) and 3 μg ml^{-1} (antisense *Uchl1*) at 60 °C for 16 h. For biotinylated RNA detection, streptavidin-HRP (Amersham Bioscience) was used (1:250) for 2 h in TNB buffer (Tris HCl pH 7.5 100 mM, NaCl 150 mM, 0.5% blocking reagent), and signals were visualized using the TSA Cy3 system (Perkin Elmer) after washing in TNT buffer (Tris HCl pH 7.5 100 mM, NaCl 150 mM, 0.05% Tween-20). *In situ* hybridization on DIG-labelled probe was performed with monoclonal anti-DIG antibody after TSA reaction. To combine RNA *in situ* hybridization with immunofluorescence, slices were incubated with anti-tyrosine hydroxylase (TH) antibody 1:1,000 (Chemicon). Signals were then detected with fluorescent dye-conjugated secondary antibody goat anti-rabbit 405 and goat anti-mouse 488. Sections were then washed, mounted with Vectashield (Vector lab) mounting medium and observed with a confocal microscope (Leica).

Western blot. Cells were lysed in SDS sample buffer 2×. Proteins were separated in 15% SDS– polyacrylamide gel and transferred to nitrocellulose membranes. Immunoblotting was performed with the following primary antibodies: anti-UCHL1 (3524 Cell Signaling), anti-UXT (11047-1-AP Proteintech Group), anti-p53 (1C12) monoclonal antibody (2524, Cell Signaling) and anti-β-actin (A5441, Sigma). For the mTOR pathway: anti-phospho-p70 S6 kinase (Thr 389) (9234), anti-phospho-4E-BP1 (Ser 65) (9451), anti-p70 S6 kinase (9202), anti-4E-BP1 (9452), anti-phospho-Akt (Ser 473) (3787) were all purchased from Cell Signaling. Signals were revealed after incubation with recommended secondary antibodies

conjugated with horseradish peroxidase by using enhanced chemiluminescence for UCHL1 (WBKLS0500 Immobilion Western Chemioluminescent HRP substrate) and ECL detection reagent (RPN2105, GE Healthcare).

Protein stability. MN9D cells were seeded in 12-well plates overnight and then exposed to 100 μg ml^{-1} protein synthesis inhibitor cycloheximide (CHX) for 15 min and rapamycin 1 μM or DMSO vehicle control for the following 45 min.

Cellular fractionation. Nucleo-cytoplasmic fractionation was performed using Nucleo-Cytoplasmic separation kit (Norgen) according to the manufacturer's instruction. RNA was eluted and treated with DNase I. The purity of the cytoplasmic fraction was confirmed by qRT–PCR on pre-ribosomal RNA.

Polysome profiles. Polysome profiles were obtained using sucrose density gradients. MN9D cells were treated with 1 μg ml^{-1} rapamycin for 35 min, then with 100 μg ml^{-1} cycloheximide for 10 min prior to lysis in 150 μl lysis buffer (50 mM Tris-HCl pH 7.5, 100 mM NaCl, 30 mM $MgCl_2$, 100 μg ml^{-1} cycloheximide, 0.1% NP-40, 40 U ml^{-1} RNasin, protease inhibitors cocktail). Whole-cell extracts were clarified at 4 °C for 10 min at 15,000*g*. The equivalent of 5–10 absorbance units at 254 nm of the clarified cell extract was layered onto 15–55% (w/v) sucrose gradient (50 mM Tris/acetate pH 7.5, 50 mM NH_4Cl, 12 mM $MgCl_2$ and 1 mM DTT) and centrifuged for 3 h 30 min at 39,000 r.p.m. in a Beckman SW41Ti rotor at 4 °C. The gradient was pumped out by upward displacement and absorbance at 254 nm was monitored using BioLogic LP software (Bio-Rad). One-millilitre fractions were collected, 1 ml Trizol reagent (Invitrogen) was added and RNA was extracted following the manufacturer's instructions. A fixed volume of each RNA sample was then retro-transcribed and the percentage of mRNA in each fraction was calculated as relative Ct value to total RNA.

Metabolic labelling. MN9D were used for analysis of translational rate. Cells were seeded at sub-confluency in 6-well plates, and rapamycin (1 μM) or DMSO stimulations were performed for 45 min. Cells were labelled with 5 μCi ml^{-1} of [^{35}S]methionine (Amersham Pharmacia Biotech) for 45 min. Cells were lysed in standard lysis buffer (Tris-HCl 20 mM, NaCl 20 mM, 0.5% Triton X-100) and centrifuged. Supernatants were trichloroacetic-acid-precipitated and filtered on glass fibre discs under vacuum. Discs were counted with scintillation fluid in a β-counter. Total proteins were measured with the standard BCA method. Rate of incorporation was expressed as CPM/total protein ratio (mean ± s.d.). Experiments were done in triplicate.

Pulse labelling and immunoprecipitation. To monitor *de novo* protein synthesis, HEK cells were transiently transfected with pEGFP plasmid (Clontech) in combination with antisense GFP or empty control vector. After 24 h, medium was replaced with methionine/cysteine-free DMEM for 1 h. Then, cells were labelled with 100 μCi ml^{-1} of [^{35}S]methionine/cysteine (EasyTag, Perkin-Elmer) for 1 h. Labelled cells were collected, lysed in RIPA buffer (150 mM NaCl, 50 mM Tris pH 8, 1 mM EDTA, 1% NP40, 0.5% deoxycholic acid and 0.1% SDS) and used for immunoprecipitation with anti-GFP antibody (Invitrogen) overnight. Immune complexes were isolated with protein G-sepharose beads (Amersham) and separated on 10% SDS–PAGE. Newly translated GFP was visualized by autoradiography. Densitometric analysis was performed on high-resolution images with Photoshop-CS5. Normalization was obtained relative to input.

Northern blot. Polysome fractions were digested with 100 μg ml^{-1} proteinase K in 1% SDS and 10 μg glycogen (Invitrogen) at 37 °C for 1 h. RNA was obtained by phenol/chloroform extraction and re-suspended in formaldehyde/formamide MOPS buffer. Samples were incubated for 5 min at 65 °C before being loaded into formaldehyde 1% agarose gel and run at 90 V for 4 h at 4 °C. RNA was transferred onto Amersham Hybond-XL nylon membranes and UV-crosslinked. A radiolabelled *Uchl1*-specific complementary RNA probe was transcribed from the same plasmid used for *in situ* hybridization, performing the reaction in the presence of 50 μCi of α-^{32}P-UTP (Perkin-Elmer). After treatment with DNase I (Ambion), the labelled riboprobe was purified on RNeasy columns (Qiagen). Membranes were pre-hybridized for 3 h at 65 °C with NorthernMax prehybridization/hybridization buffer (Ambion) supplemented with 50 μg ml^{-1} salmon sperm DNA (Invitrogen), and hybridized with UCHL1 riboprobe overnight at 65 °C in the same buffer. After extensive washes (most stringent conditions were 0.2× SSC/0.1% SDS at 65 °C), membranes were exposed to autoradiography at −80 °C with intensifying screens.

Bioinformatic analysis. For the identification of additional translational activator candidates, we searched for FANTOM3 full-length cDNAs that were non-coding RNAs and overlap the 5′ end of coding transcripts in a head-to-head configuration. The filtered set of 8,535 FANTOM3 ncRNA transcripts described previously[30] was used as our starting point. Genomic locations of these ncRNA transcripts and RefSeq[31] coding transcripts were extracted from the alignments in the UCSC Genome browser[32] to identify a set of 788 coding-sense–non-coding-antisense pairs. ncRNAs were then checked by RepeatMasker to identify SINEB2-related sequences (http://www.repeatmasker.org). This analysis reduced the number of pairs to 127 protein-coding transcripts with overlap at the 5′ end (60 with a sense strand version of the repeat, 53 with an antisense version and 14 with both sense and antisense versions).

Alignment of the SINEB2-related elements was then carried out using Clustalw (http://www.ebi.ac.uk/Tools/clustalw2/index.html). From this analysis the antisense overlapping transcripts with a repeat most similar to the one of antisense *Uchl1* as well as in the same orientation were chosen for experimental testing (antisense *Uxt*).

Statistical analysis. Statistical analyses were performed with paired two-tailed Student's *t*-test. Results are mean ($n \geq 3$) ± standard deviation (s.d.).

27. Vandesompele, J. *et al.* Accurate normalization of real-time quantitative RT-PCR data by geometric averaging of multiple internal control genes. *Genome Biol.* **3,** RESEARCH0034 (2002).
28. Biagioli, M. *et al.* Unexpected expression of α- and β-globin in mesencephalic dopaminergic neurons and glial cells. *Proc. Natl Acad. Sci. USA* **106,** 15454–15459 (2009).
29. Ishii, T., Omura, M. & Mombaerts, P. Protocols for two- and three-color fluorescent RNA *in situ* hybridization of the main and accessory olfactory epithelia in mouse. *J. Neurocytol.* **33,** 657–669 (2004).
30. Nordström, K. J. *et al.* Critical evaluation of the FANTOM3 non-coding RNA transcripts. *Genomics* **94,** 169–176 (2009).
31. Maglott, D. R., Katz, K. S., Sicotte, H. & Pruitt, K. D. NCBI's LocusLink and RefSeq. *Nucleic Acids Res.* **28,** 126–128 (2000).
32. Kent, W. J. *et al.* The human genome browser at UCSC. *Genome Res.* **12,** 996–1006 (2002).